https://doi.org/10.5194/egusphere-2025-2080
Preprint. Discussion started: 2 June 2025

Different response characteristics of ambient hazardous trace metals and health impacts to global emission reduction

Wenwen Sun[a b c 1], Xing Liu[d 1], Rui Li[e *]

[a] *Department of Research, Shanghai University of Medicine & Health Sciences Affiliated Zhoupu Hospital, Shanghai 201318, China*

[b] *Shanghai Key Laboratory of Atmospheric Particle Pollution and Prevention (LAP[3]), Department of Environmental Science and Engineering, Fudan University, Shanghai 200433, China*

[c] *College of Medical Technology, Shanghai University of Medicine & Health Sciences, Shanghai 201318, China*

[d] *State Environmental Protection Key Laboratory of Coastal Ecosystem, National Marine Environmental Monitoring Center, Dalian 116023, China*

[e] *Key Laboratory of Geographic Information Science of the Ministry of Education, School of Geographic Sciences, East China Normal University, Shanghai, 200241, PR China*

*** Corresponding author**

Prof. Rui Li (rli@geo.ecnu.edu.cn)

[1]Wenwen Sun and Xing Liu contributed to the work equally.

Abstract

Airborne hazardous trace metals pose significant risks to human health. However, the response characteristics of ambient trace metals to emission reductions remain poorly understood. The COVID-19 pandemic offered a unique opportunity to investigate these response mechanisms and optimize emission control strategies. In this study, we employed the GEOS-Chem chemical transport model to predict global variations in atmospheric concentrations of nine hazardous trace metals (As, Cd, Cr, Cu, Mn, Ni, Pb, V, and Zn) and assess their responses to COVID-19 lockdown measures. Our results revealed that global average concentrations of As, Cd, Cr, Cu, Mn, Ni, and V decreased by 1-7%, whereas Pb and Zn levels increased by 1% and 2%, respectively. The rise in Pb and Zn concentrations during lockdowns was primarily linked to sustained coal combustion and non-ferrous smelting activities, which remained essential for residential energy demands. Spatially, India, Europe, and North America experienced the most pronounced declines in trace metal levels, while Sub-Saharan Africa and Australia showed minimal sensitivity to lockdown-induced emission

https://doi.org/10.5194/egusphere-2025-2080
Preprint. Discussion started: 2 June 2025

reductions. Based on the scenario analysis, we found the concentrations of trace metals displayed linear response to emission reduction. Combined with the health risk assessment, we demonstrated the reduced emissions of Pb and As during the lockdown period yielded the greatest health benefits—Pb reductions were associated with lower non-carcinogenic risks, while As declines contributed most significantly to reduced carcinogenic risks. Targeting fossil fuel combustion should be prioritized in Pb and As mitigation strategies.

1. Introduction

With the rapid advancement of industrial development and urbanization, numerous hazardous trace metals have been released into the atmosphere (Cheng et al., 2015; Yu et al., 2012; Zhu et al., 2020). These toxic elements injected into the air can negatively impact terrestrial and aquatic ecosystems through dry or wet deposition and pose significant risks to human health through long-term exposure (Al-Sulaiti et al., 2022; Pan and Wang, 2015; Sharma et al., 2023). Certain trace elements, including arsenic (As), cadmium (Cd), chromium (Cr), and lead (Pb), have been classified as carcinogens by the International Agency for Research on Cancer (IARC) (Bai et al., 2023; Loomis et al., 2018; Pearce et al., 2015). Therefore, it is crucial to investigate the spatiotemporal characteristics of hazardous trace metals in the atmosphere and assess their health impacts. Such efforts are instrumental in identifying hotspots and formulating effective control measures to mitigate health risks.

A growing body of studies have explored the long-term trends of ambient trace elements in various cities (Das et al., 2023; Guo et al., 2022; Nirmalkar et al., 2021). For example, Farahani et al. (2021) reported significant decreases in $PM_{2.5}$-bound levels of nickel (Ni), vanadium (V), zinc (Zn), lead (Pb), manganese (Mn), and copper (Cu) in central Los Angeles between 2005 and 2018 (Farahani et al., 2021). Very recently, Li et al. (2022) confirmed that concentrations of Pb, zinc (Zn), and arsenic (As) in $PM_{2.5}$ in Tangshan decreased by 62%, 59%, and 54% from 2017 to 2020, respectively, owing to the implementation of clean air actions. Although some studies have analyzed the long-term trends of ambient hazardous trace metals in specific regions, the spatiotemporal variations in most areas remain poorly understood due to the limited spatial representativeness of monitoring sites. To address these limitations, some researchers have utilized chemical transport models to predict regional or global concentrations of ambient hazardous trace metals. For instance,

https://doi.org/10.5194/egusphere-2025-2080
Preprint. Discussion started: 2 June 2025

Liu et al. (2021) employed the CMAQ model to estimate the concentrations of 11 trace elements and found that most of these elements exhibited higher levels in the North China Plain (NCP). Additionally, Zhang et al. (2020) used the GEOS-Chem model to predict global ambient arsenic (As) concentrations from 2005 to 2015. Their findings revealed that atmospheric As levels in India exceeded those in eastern China, primarily due to the sharp increase in coal combustion across India. However, to date, the spatiotemporal variations of multiple hazardous trace metals on a global scale remain poorly understood. Moreover, the response of ambient trace elements to changes in emissions is still unknown. Bridging this knowledge gap is crucial for implementing effective control and prevention measures targeted at specific trace elements.

COVID-19 swept across the globe between January and April 2020 (Fonseca et al., 2021; Saadat et al., 2020; Venter et al., 2020). To prevent the rapid spread of this complex disease, many strict lockdown measures were implemented, including the partial or complete closure of international borders, the shutdown of nonessential businesses, and restrictions on citizen mobility (Meo et al., 2020; Onyeaka et al., 2021; Xing et al., 2021). These stringent control measures led to dramatic decreases in the levels of many gaseous precursors, such as NO_x and CO. Keller et al. (2021) estimated that global NO_x emissions were reduced by 3.1 Tg N during January-June 2020, accounting for 5.5% of total anthropogenic emissions. In addition, many studies have analyzed the response mechanisms of secondary pollutants to emission reductions during this period. Li et al. (2023b) identified three distinct response mechanisms of secondary nitrogen-bearing components to the reduction in NO_x emissions. Although the impacts of COVID-19 lockdown on multiple pollutants have been explored, the response of ambient hazardous trace metals to emission changes during the COVID-19 period still remains unknown. Additionally, the separate contributions of emission reductions and meteorological factors to ambient hazardous trace metal levels are also unclear. The COVID-19 pandemic provided an unprecedented opportunity to uncover these response mechanisms and marginal benefits of emission reduction, offering valuable insights for developing effective air pollution mitigation strategies.

Here, we developed a new trace metal emission inventory and employed the GEOS-Chem model to predict the global variations of ambient trace elements before and during the COVID-19 period. First, we analyzed the spatiotemporal variations of ambient trace metal levels. Then, we

https://doi.org/10.5194/egusphere-2025-2080
Preprint. Discussion started: 2 June 2025

distinguished the contributions of emission changes and meteorology. Finally, we quantified the health benefits resulting from emission reductions. Our study provides valuable insights and targeted policy implications for future air pollution control.

2. Materials and methods

2.1 The global emission inventory of hazardous trace metals

According to the classification standard proposed by Streets et al. (2011), all countries and regions worldwide could be categorized into five groups, ranging from the most developed (Region 1) to the least developed (Region 5). Anthropogenic emission factors and the removal efficiency of hazardous trace metals vary significantly among these regions. Detailed data were obtained from Zhu et al. (2020). Coal combustion sources were further divided into two subcategories: coal-fired power plants and other coal-fired sectors. Non-coal combustion sources were classified into six subsectors: liquid fuel combustion, ferrous metal smelting, non-ferrous metal smelting, non-metallic mineral manufacturing, vehicle emissions, and municipal solid waste incineration. Natural emissions, including those from dust, biomass burning, and sea salt, were estimated in detail using the methodology described by Wu et al. (2020). Based on these categorizations and methodologies, an emission inventory for nine trace metals including As, Cd, Cr, Cu, Mn, Ni, Pb, V, and Zn was developed. The detailed emission inventory description was introduced in Supporting Information.

2.2 Ground-level observations

Most of the ground-level ambient hazardous trace metal observations (PM_{10}) mainly focused on China, Western Europe, and Contiguous United States. China did not possess regular ground-level observations of ambient trace metals, and thus we only collected these data from previous references. Both of Western Europe and Contiguous United States possessed regular ambient trace metal observations. The European Monitoring and Evaluation Programme (EMEP) comprises of more than 100 sites about trace metal observations across Europe in past 20 years. The quality control of EMEP was explained by Tørseth et al., (2012). The dataset of daily ambient trace metal concentrations in many sites across the United States were downloaded from the website of https://www.epa.gov/ (Figure S1).

2.3 GEOS-Chem model

The GEOS-Chem model (v12-01) was utilized to simulate the concentration differences of nine

https://doi.org/10.5194/egusphere-2025-2080
Preprint. Discussion started: 2 June 2025

hazardous trace metals in the atmosphere during the period from January 23 to April 30, comparing 2020 to 2019. These differences were attributed to the combined effects of emission changes and meteorological variations. The core mechanism of this model integrates tropospheric NOx-VOC-O3-aerosol chemistry (Mao et al., 2010; Park et al., 2004). Wet deposition processes include sub-grid scavenging in convective updrafts, in-cloud rainout, and below-cloud washout (Liu et al., 2001). Dry deposition was calculated using a resistance-in-series model (Wesely, 2007). The model was driven by meteorological data assimilated from the MERRA2 reanalysis (Qiu et al., 2020). A global simulation at a 2 × 2.5° resolution was conducted to estimate the concentrations of hazardous trace metals on a global scale (Qiu et al., 2020). Anthropogenic trace metal emission inventories for 2019 and 2020 were derived from Section 2.1, while natural emissions included dust, biomass burning, and sea salt. The modelled trace metal concentration is the sum of TE concentrations in particle sizes≤2.5 μm in diameter (accumulation mode) and particle sizes between 2.5 and 10 μm in diameter (coarse mode). Model performance was evaluated using several statistical indicators, with the detailed equations provided in the Supplementary Information (SI).

To isolate the effects of emission reductions and meteorological changes on ambient hazardous trace metals, simulations using the 2019 emission inventory and 2020 meteorological conditions ($GC_{2019emi\text{-}2020met}$) were also conducted. GC_{2020} and GC_{2019} represent simulation results based on the emissions and meteorological conditions of 2020 and 2019, respectively. The pollutant concentration differences between 2019 and 2020 caused by emissions (GC_{emi}) and meteorology (GC_{met}) were quantified using the following equations:

$$GC_{emi} = GC_{2020} - GC_{2019emi-2020met} \quad (1)$$
$$GC_{met} = GC_{2019emi-2020met} - GC_{2019} \quad (2)$$

The detailed calculation process is as follows. First, the concentrations of ambient trace metals for both 2019 and 2020 were simulated. In the second step, the meteorology for 2020 was fixed, and the emission inventory was adjusted to 2019 to calculate $GC_{2019emi\text{-}2020met}$. The simulated ambient trace metal levels for 2020 were then subtracted from the simulated concentrations with 2019 emissions and 2020 meteorology (Eq. 1) to determine the contribution of emissions to the total difference in ambient trace metals during the COVID-19 period (GC_{emi}). Similarly, based on Eq. 2, the same method was applied to estimate the contribution of meteorology to the total difference in

https://doi.org/10.5194/egusphere-2025-2080
Preprint. Discussion started: 2 June 2025

ambient trace metals during the COVID-19 period (GC_{met}). Different regions exerted lockdown measures during different periods. The lockdown periods in various regions were collected from https://en.wikipedia.org/wiki/COVID-19_pandemic_lockdowns (Keller et al., 2021). Five scenarios including base, 20%_reduction, 40%_reduction, 60%_reduction, and 80%_reduction were set up to assess the response of trace metal concentrations to emission change. For example, the 20%_reduction means the global trace metal emission experienced 20% reduction.

2.4 Health risk assessment model

In this study, the carcinogenic and non-carcinogenic risks associated with hazardous trace metals in aerosols were evaluated using statistical thresholds established by IARC. Based on the IARC classification, trace metals such as As, Cd, Cr, Cu, Mn, Ni, Pb, V, and Zn are identified as potentially carcinogenic to humans (Marufi et al., 2024; Tikadar et al., 2024). The risks of exposure to these hazardous trace metals were assessed for both adults (⩾24 years old) and children (<6 years old) using carcinogenic risk (CR) and hazard quotient (HQ) metrics. Both CR and HQ were derived from the average daily dose (ADD). The formulas used to calculate ADD, CR, and HQ were adopted from Kan et al. (2021) and Zhang et al. (2021) (Table S1-S2):

$$ADD=(C\times InhR\times EF\times ED)/(BW\times AT) \quad (3)$$

$$HQ=ADD/RfD \quad (4)$$

$$CR = ADD\times CSF \quad (5)$$

where C (mg m^{-3}) represents the concentration of hazardous trace metals in the atmosphere, whereas InhR denotes the respiratory rate (m^3 d^{-1}) (Table S1). EF refers to the annual exposure frequency (d y^{-1}), ED is the exposure duration (years), BW represents the average body weight (kg), and AT is the average exposure time (days). ADD indicates the average daily intake (mg kg^{-1} d^{-1}) of hazardous trace metals, RfD is the reference dose (mg kg^{-1} d^{-1}) derived from reference concentrations, and CSF is the cancer slope factor (kg d mg^{-1}). The potential non-carcinogenic risk of hazardous trace metals is considered high if the hazard quotient (HQ) exceeds 1.0, indicating significant health concerns. Conversely, an HQ below 1.0 suggests negligible health risks. The carcinogenic risk (CR) of each hazardous trace metal is assessed as significant if CR exceeds 10^{-4}.

3. Results and discussions

3.1 Model evaluation

https://doi.org/10.5194/egusphere-2025-2080
Preprint. Discussion started: 2 June 2025

Initially, the GEOS-Chem model was employed to estimate ambient trace metal concentrations at the global scale. The correlation coefficients (R values) between the simulated and observed values for As, Cd, Cr, Cu, Mn, Ni, Pb, V, and Zn were 0.76, 0.75, 0.81, 0.75, 0.79, 0.81, 0.83, 0.78, and 0.79 (Figure 1), respectively. The root mean square errors (RMSE) for As, Cd, Cr, Cu, Mn, Ni, Pb, V, and Zn were 2.57, 4.45, 4.84, 11.1, 12.7, 3.64, 28.1, 9.33, and 30.1 ng/m^3, respectively. The mean absolute errors (MAE) for these trace metals were 0.92, 2.89, 2.15, 5.53, 6.73, 1.60, 12.3, 4.09, and 13.5 ng/m^3, respectively. Only Ni and V were overestimated, while the concentrations of most other trace metals were slightly underestimated. The predictive R values in our study were generally higher than those reported by Liu et al. (2021), with the exception of Mn (R = 0.87) and Cu (R = 0.86). It is likely that Liu et al. (2021) simulated ambient trace metal concentrations specifically in China, which experiences some of the most severe trace metal pollution globally. As a result, the simulated values in China were often underestimated. In contrast, our study conducted global simulations, which helped avoid such significant underestimation. Additionally, the predictive accuracy for ambient As concentrations in our study was slightly higher than that of Zhang et al. (2020) (R = 0.69). Overall, the predictive accuracy of ambient trace metal concentrations in our study was satisfactory, allowing us to use these data to further analyze the spatiotemporal characteristics of trace metal distributions.

3.2 The concentration differences and health benefits of ambient trace metals during 2019 and 2020

Based on the simulated results, the global average concentrations of ambient As, Cd, Cr, Cu, Mn, Ni, Pb, V, and Zn during January-April in 2019 (2020) were 0.05 (0.04), 0.02 (0.02), 0.12 (0.12), 0.39 (0.37), 0.21 (0.20), 0.17 (0.16), 0.82 (0.83), 0.24 (0.22), and 0.43 (0.44) ng/m^3 (Figure 2 and Figure S2-S4), respectively. Most trace metals in the atmosphere experienced decreases during the COVID-19 period in 2020 compared to the "business-as-usual" period in 2019. The global average concentrations of ambient As, Cd, Cr, Cu, Mn, Ni, and V decreased by 5%, 1%, 1%, 4%, 5%, 7%, and 7%, respectively. However, global average concentrations of particulate Pb and Zn exhibited slight increases of 1% and 2%, respectively, during the same period.

The ambient hazardous trace metals exhibited distinct spatial variations across regions during this period. Nearly all trace metal concentrations in India (Ind), Western Europe (WE), North America (NA), and Russia (Rus) showed significant decreases following the COVID-19 outbreak

https://doi.org/10.5194/egusphere-2025-2080
Preprint. Discussion started: 2 June 2025

(Figure 3). For example, particulate As concentrations in these regions decreased by 4%, 17%, 10%, and 12%, respectively. These reductions are likely linked to the high trace metal emissions during the "business-as-usual" period, driven by fossil fuel combustion for industrial activities (activity level decreased by 23%), which were substantially curtailed by stay-at-home orders (Bai et al., 2023; Doumbia et al., 2021). In China, the concentrations of As, Cu, Mn, Ni, and V decreased by 3%, 2%, 3%, 3%, and 4%, respectively. However, ambient levels of Cd, Cr, Pb, and Zn increased by 5%, 2%, 6%, and 8%, respectively. It was assumed that most of these trace metals were mainly derived from residential fossil fuel combustion (increase by 5%) and essential industrial emissions (remained relatively stable) (Zhu et al., 2020; Zhu et al., 2018), which even increased due to the stay-at-home order. In South America (SA), most trace metals, except for As and Mn, showed slight decreases during the COVID-19 period. Conversely, ambient trace metal concentrations in Sub-Saharan Africa (SS) and Australia (Aus) were relatively insensitive to COVID-19 lockdown measures, remaining stable throughout the period. It was supposed that the concentrations of trace metals in these regions were relatively low during the "business-as-usual" period.

Although the absolute concentrations provide an overall indication of the impact of lockdown measures on ambient trace metals, the contribution of meteorological factors cannot be disregarded. Meteorological conditions can significantly influence ambient trace metal concentrations, potentially complicating the interpretation of trace metal responses to emission changes. To isolate this effect, we applied the isolation technique to separate the contributions of emission changes from those of meteorological factors. At the global scale, most ambient trace metal concentrations, except for Pb and Zn, showed slight decreases, reflecting minor emission reductions coupled with favorable meteorological conditions that decreased concentrations (Figure 4 and Figure S5-S12). However, the slight increases in Pb and Zn concentrations were likely due to the fact that favorable meteorological conditions could not offset the significant rise in emissions of these metals during the period. It is assumed that Pb and Zn were primarily derived from coal combustion and non-ferrous smelting industries (Li et al., 2023a). In our study, the global residential energy consumption even increased by 5% during COVID-19 period based on the statistical data (https://www.iea.org/), which could lead to slight increases of Pb and Zn concentrations. Previous studies also have confirmed that residential coal consumption increased notably (10-20%) during the lockdown period (Li et al., 2021; Smith et al., 2021). Emission changes and meteorological conditions exhibited significant spatial heterogeneity. In China, overall meteorological conditions favored trace metal removal, though unfavorable conditions in northern Hebei Province and Northeast China during January 2020 limited this effect (Chang et al., 2020; Huang et al., 2020; Li et al., 2023b). Most regions, such as South China and West China, experienced favorable meteorological conditions, as confirmed by several studies (Li et al., 2023b). Despite this, emission-induced concentrations of Cd, Cr, Pb, and Zn in China still showed slight increases during the COVID-19 period, suggesting that essential sectors, such as coal and non-ferrous industries, could not be fully shut down. The data of National Bureau of Statistics (https://data.stats.gov.cn/index.htm) also verified that the coal consumption and products of non-ferrous industries in China nearly remained invariable during this period. In regions like India, WE, NA, and Russia, favorable meteorological conditions combined with substantial emission reductions led to decreases in most trace metal concentrations. Keller et al. (2021) demonstrated that stay-at-home orders in WE and parts of NA resulted in more than a 50% reduction in NO_x emissions (mainly from vehicle emission and industrial activity), a trend consistent with the trace metal reductions observed in our study. In SA, the emission-induced reductions of trace metals were more pronounced than those due to meteorological conditions. This might be because countries such as Chile and Brazil have relatively high non-essential trace metal emissions, which were strongly affected by lockdown measures (Huber et al., 2016; La Colla et al., 2021; Zhu et al., 2020). In SS, emission-induced reductions also exceeded meteorological effects for most trace metals, except for Mn and Ni. However, in Australia, emission-induced reductions were less significant compared to SA and SS. Despite its developed mineral mining industries, Australia has more effective pollution control measures, resulting in lower total trace metal emissions (Zhu et al., 2020; Pacyna and Pacyna, 2001; Zhou et al., 2015).

In order to assess the response of trace metal concentrations to assumed emission change, the five emission scenarios (base (annual average concentration in 2019), 20%, 40%, 60%, and 80%) were set up to evaluate the impact of emission reduction. In our study, the results suggested that the As concentrations in China, India, WE, NA, SA, SS, Russia, and Australia decreased from 1.14, 0.55, 0.13, 0.09, 0.04, 0.01, 0.08, and 0.01 to 0.23, 0.11, 0.03, 0.02, 0.01, 0, 0.02, and 0 ng/m^3 (Figure S13a), respectively. Besides, concentrations of other trace metals also displayed linear

https://doi.org/10.5194/egusphere-2025-2080
Preprint. Discussion started: 2 June 2025

decreases with the increasing of emission reduction ratio (Figure S13). It was assumed that these trace metals did not participate in chemical reactions in the atmosphere and were only affected by physical processes.

3.3 Unexpected health benefits from COVID-19 period

Based on the equations of (3)-(5), the global health risk indicators including CR (carcinogenic risk) and HQ (hazard quotient) values were calculated. At the global scale, among all of the trace metals, Pb showed the highest CR values (9.7×10^{-8} and 2.4×10^{-7}), followed by Ni (3.5×10^{-8} and 8.6×10^{-8}), Cd (3.0×10^{-8} and 7.2×10^{-8}), As (1.6×10^{-8} and 3.9×10^{-8}), and Cr (1.4×10^{-8} and 3.4×10^{-8}), and the lowest ones for Cu, Mn, V, and Zn in both of 2019 and 2020. For non-carcinogenic risk, HQ values showed the higher values for As (3.5×10^{-5} and 9.0×10^{-5}) and Cu (2.2×10^{-5} and 5.5×10^{-5}). The results were in good agreement with previous studies because As often showed the higher non-carcinogenic risk (Li et al., 2023).

The CR and HQ values can be summed to estimate the total carcinogenic and non-carcinogenic risks. By comparing the CR and HQ values between 2019 and 2020, we quantified the health burden (or benefits) attributable to the COVID-19 lockdown (Figure 5 and Figure S14-S15). At the spatial scale, significant decreases in health burden were observed across most regions of the NCP, Southeast China, WE, the Dun River Basin, and the eastern United States. Following January 23, 2020, at least 29 provinces in China reported confirmed COVID-19 cases. In response, strict control measures, including the shutdown of commercial activities and the lockdown of entire cities, were implemented. These measures significantly reduced emissions, particularly in populous regions such as the NCP and Southeast China (Jia et al., 2021; Shi and Brasseur, 2020). Similarly, in New York, stay-at-home orders and social restrictions were rigorously enforced by late March 2020 (Tzortziou et al., 2022). These interventions contributed to substantial reductions in trace metal emissions, thereby mitigating associated health damages. In contrast, notable increases in health burden were observed in Northeast China, the southern coastal regions of China, and certain scattered areas in the Middle East. The rise in health risks linked to trace metal exposure in Northeast China and southern coastal regions may be associated with pollution aggravation during the COVID-19 period (Huang et al., 2021). Previous studies have highlighted that these regions experienced persistent air pollution or increased metal concentrations during the lockdown,

https://doi.org/10.5194/egusphere-2025-2080
Preprint. Discussion started: 2 June 2025

primarily due to unfavorable meteorological conditions (Li et al., 2023b). For instance, the prevalence of stable weather patterns, such as reduced wind speeds and atmospheric stagnation, significantly elevated ambient trace metal concentrations (McClymont and Hu, 2021; Şahin, 2020).

In our study, the global regions were categorized into eight major domains. During the COVID-19 period, China and India demonstrated the highest health benefits resulting from reductions in trace metal emissions. Additionally, Europe, NA, and Russia also exhibited significant health benefits. In contrast, SA, SS, and Australia showed the lowest health benefits, with some areas even experiencing an increase in health burden following the COVID-19 outbreak. The ambient trace metals in SA, SS, and Australia appeared to be less sensitive to lockdown measures due to relatively low baseline trace metal exposures in these regions. Combined the response of trace metal concentration to emission reduction in five scenarios, we also demonstrated that trace metal emission reductions are most effective in mitigating health damages in regions with high baseline exposures, such as China and India. Future efforts to target emission reductions in these regions could yield substantial public health benefits.

4 Conclusions and implications

The global lockdowns during the COVID-19 pandemic significantly reduced anthropogenic emissions, yet the response of ambient trace metal concentrations to these control measures remains insufficiently understood. In this study, we developed an updated global trace metal emission inventory and employed a chemical transport model to predict the concentrations of nine trace metals for January-April in 2019 and 2020. Our results revealed that the response characteristics of trace metals to lockdown measures varied substantially. Global average concentrations of ambient As, Cd, Cr, Cu, Mn, Ni, and V decreased by 5%, 1%, 1%, 4%, 5%, 7%, and 7%, respectively, following the COVID-19 outbreak. However, global average concentrations of particulate Pb (1%) and Zn (2%) showed slight increases during the same period. This trend can be attributed to coal combustion and non-ferrous smelting industries, which are critical sectors for meeting residential needs and thus less responsive to emission control measures. Significant spatial variations in trace metal responses to lockdown measures were also observed. For instance, lockdown interventions were more effective in reducing trace metal pollution in India, Europe, and NA compared to other regions. Moreover, the trace metal concentrations show the linear response to emission reduction,

https://doi.org/10.5194/egusphere-2025-2080
Preprint. Discussion started: 2 June 2025

and thus the prioritizing emission reductions in heavily polluted areas (e.g., China, India, WE, and NA) yields higher marginal benefits and greater public health gains. From a health burden perspective, controlling emissions of Pb and As emerged as the most effective strategies for mitigating carcinogenic and non-carcinogenic risks, respectively. Both elements are primarily associated with fossil fuel combustion, particularly coal burning. However, the persistent increase in energy consumption poses a challenge to achieving meaningful reductions in Pb and As emissions. In the future, it will be essential to implement additional control measures to curb Pb and As emissions during coal combustion processes, thereby maximizing health benefits and reducing environmental risks.

It is important to acknowledge several limitations in our study. Firstly, the simulated concentrations of hazardous trace metals in SA and SS might contain uncertainties due to the scarcity of ground-level observations in these regions. This lack of observational data makes it challenging to accurately evaluate the predictive reliability of ambient trace metal concentrations in these areas. Consequently, these uncertainties may also propagate to the health risk assessments. To address this, it is crucial to establish more monitoring sites for ambient trace metals in SA and SS. Secondly, the health risk assessment in this study was based solely on trace metal concentrations, without considering population exposure. In reality, health impacts are closely tied to population size and distribution. Future research should prioritize the development of more accurate methodologies that incorporate population exposure to better assess the health impacts of ambient trace metal exposure.

Acknowledgements

This work was supported by the Opening Project of Shanghai Key Laboratory of Atmospheric Particle Pollution and Prevention (LAP3) [grant numbers FDLAP24002]; Academic Mentorship for Scientific Research Cadre Project [grant numbers AMSCP-24-05-03].

Author Contributions

Conceptualization: RL, Data Curation: WS and XL, Formal analysis: RL.

Competing interests

The contact author has declared that none of the authors has any competing interests.

https://doi.org/10.5194/egusphere-2025-2080
Preprint. Discussion started: 2 June 2025

Figure 1 The predictive accuracy of nine trace metals including As (a), Cd (b), Cr (c), Cu (d), Mn (e), Ni (f), Pb (g), V (h), and Zn (i) at the global scale based on GEOS-Chem model (Unit: ng/m^3).

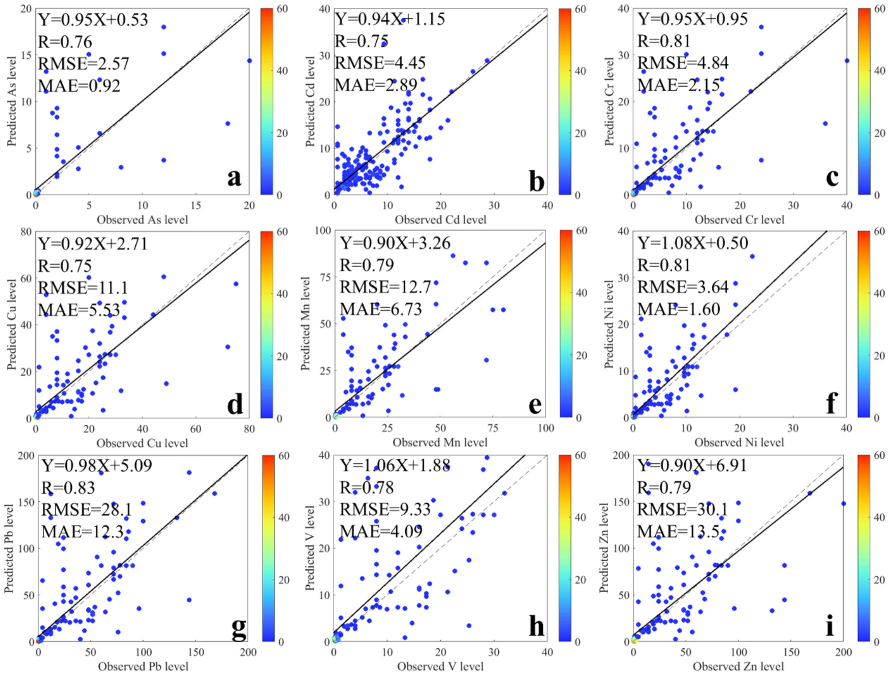

https://doi.org/10.5194/egusphere-2025-2080
Preprint. Discussion started: 2 June 2025

Figure 2 The global difference of trace element concentrations between January-April in 2019 and 2020. Nine trace elements including As (a), Cd (b), Cr (c), Cu (d), Mn (e), Ni (f), Pb (g), V (h), and Zn (i) were selected to analyze the annual variations (Unit: ng/m^3).

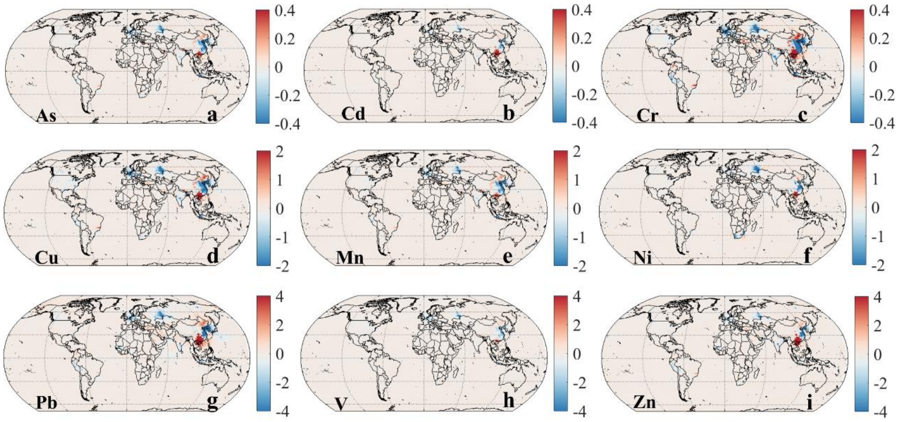

https://doi.org/10.5194/egusphere-2025-2080
Preprint. Discussion started: 2 June 2025

Figure 3 The violin graphs of nine trace elements including As (a), Cd (b), Cr (c), Cu (d), Mn (e), Ni (f), Pb (g), V (h), and Zn (i) in eight major regions during January-April in 2020. Chi, Ind, WE, NA, SA, SS, Rus, and Aus represent China, India, Western Europe, North America, South America, Sub-Sahara Africa, Russia, and Australia, respectively.

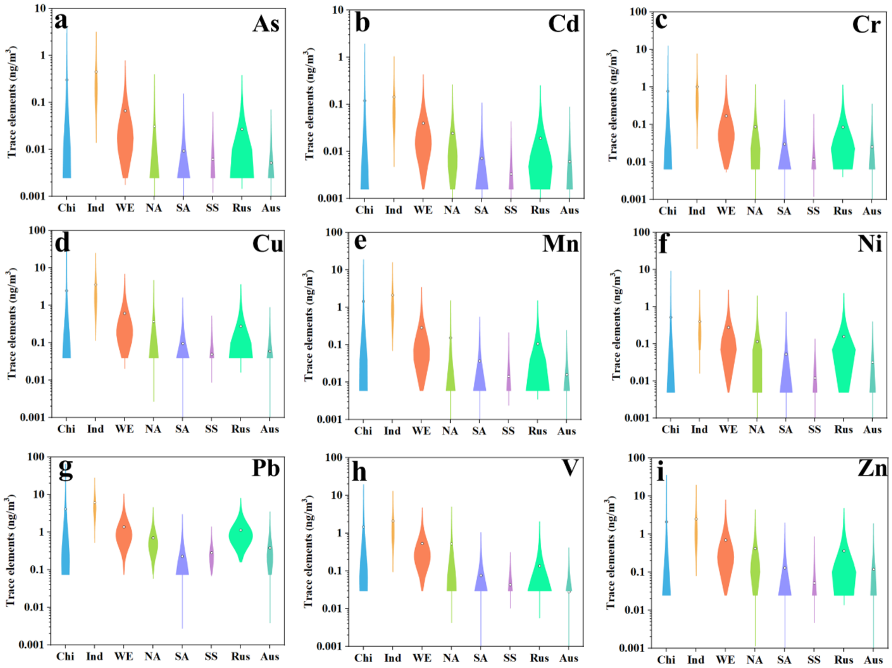

https://doi.org/10.5194/egusphere-2025-2080
Preprint. Discussion started: 2 June 2025

Figure 4 The emission and meteorological contributions to ambient As concentrations during 2019-2020 at global and eight major regions. Chi, Ind, WE, NA, SA, SS, Rus, and Aus represent China, India, Western Europe, North America, South America, Sub-Sahara Africa, Russia, and Australia, respectively.

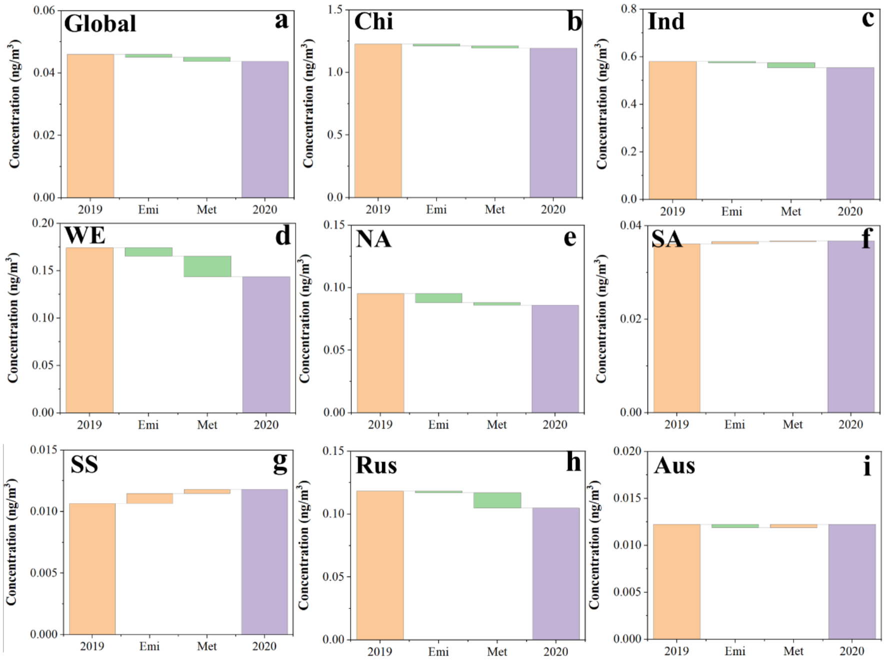

https://doi.org/10.5194/egusphere-2025-2080
Preprint. Discussion started: 2 June 2025

Figure 5 The total CR and HQ differences of adults and children for all of the nine hazardous trace metals during January-April in 2019 and 2020 (the minus of CR and HQ values in 2020 and those in 2019).

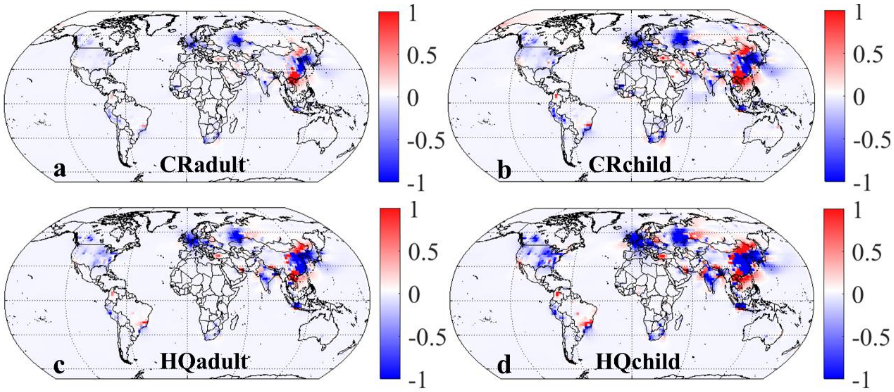

References

Al-Sulaiti, M.M., Soubra, L., Al-Ghouti, M.A. (2022) The causes and effects of mercury and methylmercury contamination in the marine environment: A review. Current Pollution Reports 8, 249-272.

Bai, X., Tian, H., Zhu, C., Luo, L., Hao, Y., Liu, S., Guo, Z., Lv, Y., Chen, D., Chu, B. (2023) Present knowledge and future perspectives of atmospheric emission inventories of toxic trace elements: a critical review. Environmental science & technology 57, 1551-1567.

Chang, Y., Huang, R.J., Ge, X., Huang, X., Hu, J., Duan, Y., Zou, Z., Liu, X., Lehmann, M.F. (2020) Puzzling haze events in China during the coronavirus (COVID-19) shutdown. Geophysical Research Letters 47, e2020GL088533.

Cheng, K., Wang, Y., Tian, H., Gao, X., Zhang, Y., Wu, X., Zhu, C., Gao, J. (2015) Atmospheric emission characteristics and control policies of five precedent-controlled toxic heavy metals from anthropogenic sources in China. Environmental science & technology 49, 1206-1214.

Das, S., Prospero, J.M., Chellam, S. (2023) Quantifying international and interstate contributions to primary ambient $PM_{2.5}$ and PM_{10} in a complex metropolitan atmosphere. Atmospheric Environment 292, 119415.

Doumbia, T., Granier, C., Elguindi, N., Bouarar, I., Darras, S., Brasseur, G., Gaubert, B., Liu, Y., Shi, X., Stavrakou, T. (2021) Changes in global air pollutant emissions during the COVID-19 pandemic: a dataset for atmospheric modeling. Earth System Science Data 13, 4191-4206.

Farahani, V.J., Soleimanian, E., Pirhadi, M., Sioutas, C. (2021) Long-term trends in concentrations and sources of $PM_{2.5}$-bound metals and elements in central Los Angeles. Atmospheric Environment 253, 118361.

Fonseca, E.M.d., Nattrass, N., Lazaro, L.L.B., Bastos, F.I. (2021) Political discourse, denialism and leadership failure in Brazil's response to COVID-19. Global public health 16, 1251-1266.

Guo, F., Tang, M., Wang, X., Yu, Z., Wei, F., Zhang, X., Jin, M., Wang, J., Xu, D., Chen, Z. (2022) Characteristics, sources, and health risks of trace metals in PM2. 5. Atmospheric Environment 289, 119314.

Huang, X., Ding, A., Gao, J., Zheng, B., Zhou, D., Qi, X., Tang, R., Wang, J., Ren, C., Nie, W. (2020) Enhanced secondary pollution offset reduction of primary emissions during COVID-19 lockdown in China. National Science Review.

Huang, X., Ding, A., Gao, J., Zheng, B., Zhou, D., Qi, X., Tang, R., Wang, J., Ren, C., Nie, W. (2021) Enhanced secondary pollution offset reduction of primary emissions during COVID-19 lockdown in China. National Science Review 8, nwaa137.

Huber, M., Welker, A., Helmreich, B. (2016) Critical review of heavy metal pollution of traffic area runoff: Occurrence, influencing factors, and partitioning. Science of the Total Environment 541, 895-919.

Jia, M., Evangeliou, N., Eckhardt, S., Huang, X., Gao, J., Ding, A., Stohl, A. (2021) Black carbon emission reduction due to COVID-19 lockdown in China. Geophysical Research Letters 48, e2021GL093243.

Kan, X., Dong, Y., Feng, L., Zhou, M., Hou, H. (2021) Contamination and health risk assessment of heavy metals in China's lead–zinc mine tailings: A meta–analysis. Chemosphere 267, 128909.

Keller, C.A., Evans, M.J., Knowland, K.E., Hasenkopf, C.A., Modekurty, S., Lucchesi, R.A., Oda, T., Franca, B.B., Mandarino, F.C., Díaz Suárez, M.V. (2021) Global impact of COVID-19 restrictions on the surface concentrations of nitrogen dioxide and ozone. Atmospheric Chemistry and Physics

https://doi.org/10.5194/egusphere-2025-2080
Preprint. Discussion started: 2 June 2025

21, 3555-3592.

La Colla, N.S., Botté, S.E., Marcovecchio, J.E. (2021) Atmospheric particulate pollution in South American megacities. Environmental reviews 29, 415-429.

Li, H., Yao, J., Sunahara, G., Min, N., Li, C., Duran, R. (2023a) Quantifying ecological and human health risks of metal (loid) s pollution from non-ferrous metal mining and smelting activities in Southwest China. Science of the Total Environment 873, 162364.

Li, R., Peng, M., Zhao, W., Wang, G., Hao, J. (2022) Measurement Report: Rapid changes of chemical characteristics and health risks for high time-resolved trace elements in PM 2.5 in a typical industrial city response to stringent clean air actions. EGUsphere 2022, 1-37.

Li, R., Zhang, L., Gao, Y., Wang, G. (2023b) Different Response Mechanisms of N-Bearing Components to Emission Reduction Across China During COVID-19 Lockdown Period. Journal of Geophysical Research: Atmospheres 128, e2023JD039496.

Li, R., Zhao, Y., Fu, H., Chen, J., Peng, M., Wang, C. (2021) Substantial changes in gaseous pollutants and chemical compositions in fine particles in the North China Plain during the COVID-19 lockdown period: anthropogenic vs. meteorological influences. Atmospheric Chemistry and Physics 21, 8677-8692.

Liu, H., Jacob, D.J., Bey, I., Yantosca, R.M. (2001) Constraints from 210Pb and 7Be on wet deposition and transport in a global three-dimensional chemical tracer model driven by assimilated meteorological fields. Journal of Geophysical Research: Atmospheres 106, 12109-12128.

Liu, S., Tian, H., Bai, X., Zhu, C., Wu, B., Luo, L., Hao, Y., Liu, W., Lin, S., Zhao, S. (2021) Significant but spatiotemporal-heterogeneous health risks caused by airborne exposure to multiple toxic trace elements in China. Environmental science & technology 55, 12818-12830.

Loomis, D., Guha, N., Hall, A.L., Straif, K. (2018) Identifying occupational carcinogens: an update from the IARC Monographs. Occupational and environmental medicine 75, 593-603.

Mao, J., Jacob, D.J., Evans, M., Olson, J., Ren, X., Brune, W., St Clair, J., Crounse, J., Spencer, K., Beaver, M. (2010) Chemistry of hydrogen oxide radicals (HO x) in the Arctic troposphere in spring. Atmospheric Chemistry and Physics 10, 5823-5838.

Marufi, N., Conti, G.O., Ahmadinejad, P., Ferrante, M., Mohammadi, A.A. (2024) Carcinogenic and non-carcinogenic human health risk assessments of heavy metals contamination in drinking water supplies in Iran: a systematic review. Reviews on Environmental Health 39, 91-100.

McClymont, H., Hu, W. (2021) Weather variability and COVID-19 transmission: a review of recent research. International Journal of Environmental Research and Public Health 18, 396.

Meo, S.A., Abukhalaf, A.A., Alomar, A.A., AlMutairi, F.J., Usmani, A.M., Klonoff, D.C. (2020) Impact of lockdown on COVID-19 prevalence and mortality during 2020 pandemic: observational analysis of 27 countries. European journal of medical research 25, 1-7.

Nirmalkar, J., Haswani, D., Singh, A., Kumar, S., Raman, R.S. (2021) Concentrations, transport characteristics, and health risks of PM2. 5-bound trace elements over a national park in central India. Journal of Environmental Management 293, 112904.

Onyeaka, H., Anumudu, C.K., Al-Sharify, Z.T., Egele-Godswill, E., Mbaegbu, P. (2021) COVID-19 pandemic: A review of the global lockdown and its far-reaching effects. Science progress 104, 00368504211019854.

Pacyna, J.M., Pacyna, E.G. (2001) An assessment of global and regional emissions of trace metals to the atmosphere from anthropogenic sources worldwide. Environmental reviews 9, 269-298.

Pan, Y., Wang, Y. (2015) Atmospheric wet and dry deposition of trace elements at 10 sites in Northern

https://doi.org/10.5194/egusphere-2025-2080
Preprint. Discussion started: 2 June 2025

China. Atmospheric Chemistry and Physics 15, 951-972.

Park, R.J., Jacob, D.J., Field, B.D., Yantosca, R.M., Chin, M. (2004) Natural and transboundary pollution influences on sulfate-nitrate-ammonium aerosols in the United States: Implications for policy. Journal of Geophysical Research: Atmospheres 109.

Pearce, N., Blair, A., Vineis, P., Ahrens, W., Andersen, A., Anto, J.M., Armstrong, B.K., Baccarelli, A.A., Beland, F.A., Berrington, A. (2015) IARC monographs: 40 years of evaluating carcinogenic hazards to humans. Environmental health perspectives 123, 507-514.

Qiu, Y., Ma, Z., Li, K., Lin, W., Tang, Y., Dong, F., Liao, H. (2020) Markedly enhanced levels of peroxyacetyl nitrate (PAN) during COVID-19 in Beijing. Geophysical Research Letters 47, e2020GL089623.

Saadat, S., Rawtani, D., Hussain, C.M. (2020) Environmental perspective of COVID-19. Science of the Total Environment 728, 138870.

Şahin, M. (2020) Impact of weather on COVID-19 pandemic in Turkey. Science of the Total Environment 728, 138810.

Sharma, A.K., Sharma, M., Sharma, A.K., Sharma, M. (2023) Mapping the impact of environmental pollutants on human health and environment: A systematic review and meta-analysis. Journal of Geochemical Exploration, 107325.

Shi, X., Brasseur, G.P. (2020) The Response in Air Quality to the Reduction of Chinese Economic Activities during the COVID-19 Outbreak. Geophysical Research Letters, e2020GL088070.

Smith, L.V., Tarui, N., Yamagata, T. (2021) Assessing the impact of COVID-19 on global fossil fuel consumption and CO_2 emissions. Energy economics 97, 105170.

Streets, D.G., Devane, M.K., Lu, Z., Bond, T.C., Sunderland, E.M., Jacob, D.J. (2011) All-time releases of mercury to the atmosphere from human activities. Environmental science & technology 45, 10485-10491.

Tikadar, K.K., Jahan, F., Mia, R., Rahman, M.Z., Sultana, M.A., Islam, S., Kunda, M. (2024) Assessing the potential ecological and human health risks of trace metal pollution in surface water, sediment, and commercially valuable fish species in the Pashur River, Bangladesh. Environmental Monitoring and Assessment 196, 1042.

Tørseth, K., Aas, W., Breivik, K., Fjæraa, A.M., Fiebig, M., Hjellbrekke, A.G., Lund Myhre, C., Solberg, S., Yttri, K.E., 2012. Introduction to the European Monitoring and Evaluation Programme (EMEP) and observed atmospheric composition change during 1972-2009. Atmos. Chem. Phys. 12, 544-5481.

Tzortziou, M., Kwong, C.F., Goldberg, D., Schiferl, L., Commane, R., Abuhassan, N., Szykman, J.J., Valin, L.C. (2022) Declines and peaks in NO< sub> 2</sub> pollution during the multiple waves of the COVID-19 pandemic in the New York metropolitan area. Atmospheric Chemistry and Physics 22, 2399-2417.

Venter, Z.S., Aunan, K., Chowdhury, S., Lelieveld, J. (2020) COVID-19 lockdowns cause global air pollution declines. Proceedings of the National Academy of Sciences 117, 18984-18990.

Wesely, M. (2007) Parameterization of surface resistances to gaseous dry deposition in regional-scale numerical models. Atmospheric Environment 41, 52-63.

Wu, Y., Lin, S., Tian, H., Zhang, K., Wang, Y., Sun, B., Liu, X., Liu, K., Xue, Y., Hao, J. (2020) A quantitative assessment of atmospheric emissions and spatial distribution of trace elements from natural sources in China. Environmental pollution 259, 113918.

Xing, X., Xiong, Y., Yang, R., Wang, R., Wang, W., Kan, H., Lu, T., Li, D., Cao, J., Peñuelas, J. (2021)

Predicting the effect of confinement on the COVID-19 spread using machine learning enriched with satellite air pollution observations. Proceedings of the National Academy of Sciences 118, e2109098118.

Yu, S., Zhu, Y.-g., Li, X.-d. (2012) Trace metal contamination in urban soils of China. Science of the Total Environment 421, 17-30.

Zhang, H., Zhang, F., Song, J., Tan, M.L., Johnson, V.C. (2021) Pollutant source, ecological and human health risks assessment of heavy metals in soils from coal mining areas in Xinjiang, China. Environmental Research 202, 111702.

Zhang, L., Gao, Y., Wu, S., Zhang, S., Smith, K.R., Yao, X., Gao, H. (2020) Global impact of atmospheric arsenic on health risk: 2005 to 2015. Proceedings of the National Academy of Sciences 117, 13975-13982.

Zhou, J., Tian, H., Zhu, C., Hao, J., Gao, J., Wang, Y., Xue, Y., Hua, S., Wang, K. (2015) Future trends of global atmospheric antimony emissions from anthropogenic activities until 2050. Atmospheric Environment 120, 385-392.

Zhu, C., Tian, H., Hao, Y., Gao, J.J., Hao, J., Wang, Y., Liu, H.J. (2018) A high-resolution emission inventory of anthropogenic trace elements in Beijing-Tianjin-Hebei (BTH) region of China. Atmospheric Environment 191, 452-462.

Zhu, C., Tian, H., Hao, J. (2020) Global anthropogenic atmospheric emission inventory of twelve typical hazardous trace elements, 1995–2012. Atmospheric Environment 220, 117061.